

# Design of a Weathering Chamber for UV Aging of Microplastics in the Mediterranean Region

Jack Galea, Anthea Agius Anastasi, and Sophie M. Briffa\*



Cite This: *ACS Omega* 2024, 9, 35627–35633

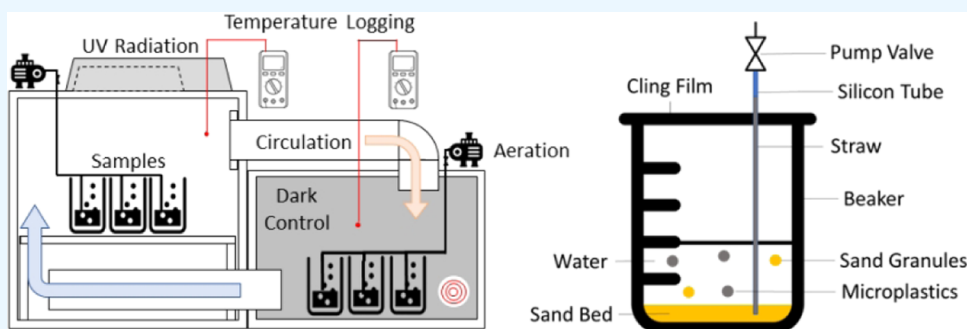


Read Online

ACCESS |

Metrics & More

Article Recommendations



**ABSTRACT:** Microplastics are an ever-growing concern in the environment. Their degradation may lead to greater absorption of toxic pollutants, which may ultimately pose a threat to human health. In the pursuit of understanding microplastics' fate, behavior, and toxicity, there is a vital need to understand their aging and weathering. For this, multiple weathering setup designs were put forward. However, standardization of a weathering setup presents a significant challenge to the field due to apparatus costs, wide range of experimental parameters, or the lack of detailed reporting. This work seeks to make much-needed data gathering more accessible by constructing a low-cost weathering chamber that simulates Mediterranean shore conditions. The weathering chamber incorporates UV irradiation, mechanical abrasion, and elevated temperatures. After extensive preliminary testing, the chamber was able to achieve the desired outcome along with UV-A irradiance values, which were similar to those in the Mediterranean.

## 1. INTRODUCTION

Polymers released into the environment are subjected to various environmental conditions, leading to fragmentation into microplastics. The ever-growing presence of microplastics within the environment has consequently led to greater organism and human exposure. Studies within the last five years have shown that microplastics are ubiquitous within the human diet, having been found in commercial salt,<sup>1</sup> drinking water,<sup>2</sup> beer, soft drinks,<sup>3</sup> mussels,<sup>4</sup> and even within fruits and vegetables.<sup>5</sup> While their effects on human health are still being analyzed,<sup>6</sup> exposure has been correlated to increased hypersensitivity<sup>7</sup> and adverse birth consequences.<sup>8</sup>

To understand these effects, the scientific community replicates behavioral changes that plastics undergo during degradation. In shore environments, these changes mainly include photooxidation, hydrolysis, mechanical abrasion, and biodegradation. Photooxidation and hydrolysis cause chain scission of the polymer backbone, leading to chemical and physical changes that are limited to the surface. Thus, mechanical abrasion by sand particles plays an important role in exposing fresh surfaces to further degradation. These three abiotic processes typically act as the initiator for

biodegradation,<sup>9</sup> fragmenting the polymer chains until they are short enough to pass through microbial cell walls.<sup>10</sup>

The Joint Group of Experts on the Scientific Aspects of Marine Environmental Protection had drawn the conclusion that up until 2016, the degradation of different plastics under specific weathering conditions was poorly understood.<sup>11</sup> By 2018, Science Advice for Policy by European Academies highlighted that weathering conditions such as UV, temperature, and oxygen availability are clear contributors to microplastic degradation. However, the main processes and time scales of such weathering are only partially known.<sup>12</sup> Such gaps have arisen from the difficulty of comparing results between weathering studies, stemming from a lack of reliably comparable weathering data for a particular plastic or incomplete reporting of weathering parameters. This issue is affirmed by recent works,<sup>13,14</sup> which proposed their own

**Received:** April 18, 2024

**Revised:** June 25, 2024

**Accepted:** July 11, 2024

**Published:** August 7, 2024



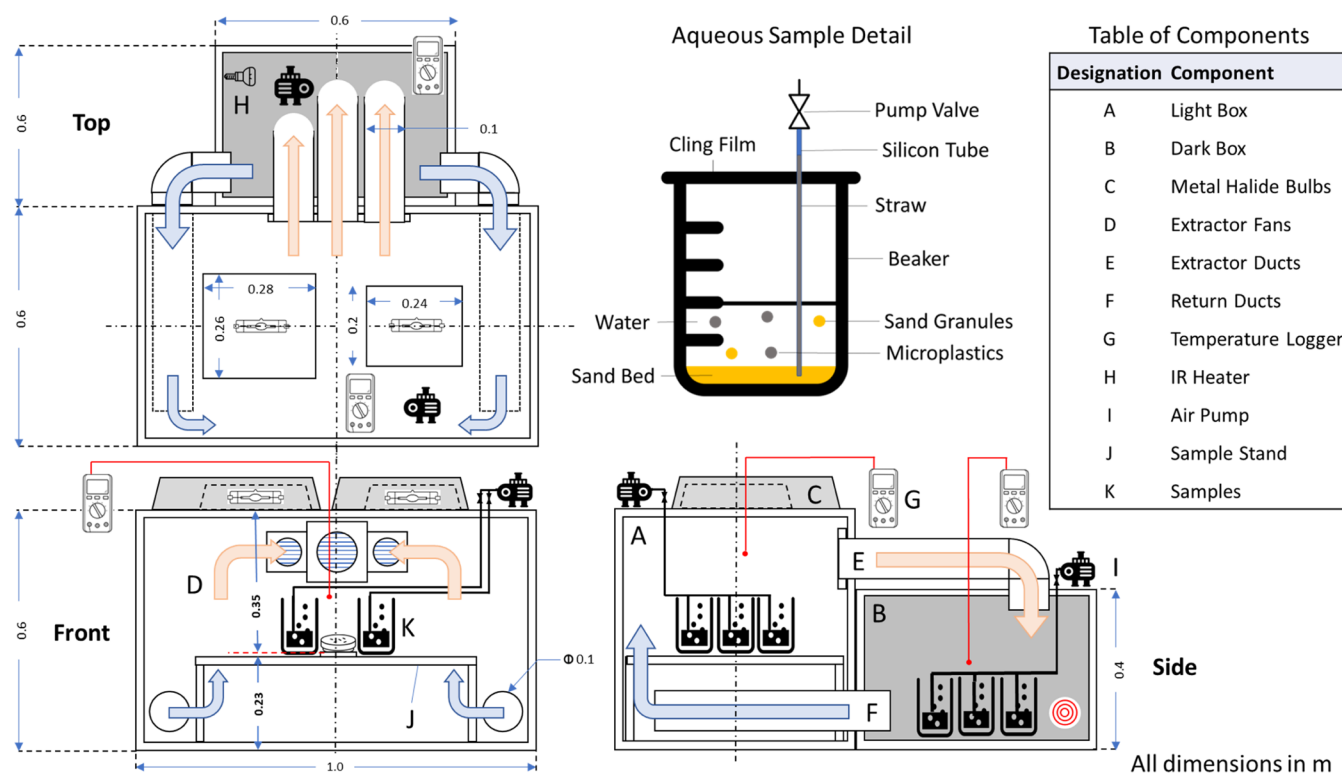


**Figure 1.** Illustration of the weathering chamber employed in this study.

guidelines in an attempt to reach a common consensus for reproducibility and comparison. The most recent challenges in weathering harmonization were summarized by Alimi et al.,<sup>15</sup> who noted that weathering parameters varied greatly, are not reported precisely, or are not clearly justified. Additionally, 51% of studies did not report the temperature at which weathering was conducted.<sup>15</sup> Interest in existing American Society for Testing and Materials standards focusing on polymer degradation has therefore surged in recent years.<sup>15</sup> However, such standards were developed long before research in microplastics emerged and are more concerned with assessing whether a product will maintain its mechanical properties after a weathering test rather than analyzing the fragmentation of any microplastics from bulk.

From this lack of harmonization, three main experimental setups have emerged to conduct microplastic weathering, as summarized by Andrade et al.<sup>16</sup> Field experiments, where plastics are deployed in the natural environment, produce the most realistic results in local conditions, but are the least reproducible.<sup>16</sup> Artificial weathering chambers provide excellent control over the experimental parameters. However, they are limited by cost and sample mounting restrictions which limit immersion in aquatic environments and exposure to mechanical abrasion.<sup>15</sup> Thus, Andrade et al.<sup>16</sup> proposed ad hoc setups as a compromise between the previous two approaches. Such setups can simulate natural conditions adequately, are adaptable to different local conditions, and are accessible at a low cost.

Therefore, the aim of this work was to develop an ad hoc weathering chamber that could be easily modified to replicate the environmental shoreline conditions of Malta and, by extension, the Mediterranean. This was specifically achieved by improving on the setup proposed by Andrade et al.<sup>16</sup> This in turn, contributes toward making microplastic weathering

setups more accessible for the field and facilitating data gathering.

## 2. METHODOLOGY: DESIGN AND TESTING OF THE CHAMBER

The following section describes each stage of the construction process of the weathering chamber. To ensure that the final setup would simulate solar conditions for the Mediterranean, irradiance readings were taken throughout each stage. For all stages, 20 readings were taken using an OPTIMUM SRI-2000 Spectral Light Meter.

**2.1. Understanding Bulb Behavior in Different Conditions.** The first step involved understanding the behavior of the bulb with respect to irradiance and different setup conditions. This was done to eventually determine the number of metal halide bulbs and optimum sample distance required for the setup, and therefore, the final width and height of the chamber, respectively. A stand was constructed to hold a single bulb fixture facing downward at height intervals of 10 cm. A spectral light meter was laid directly under the fixture, facing up toward the fixture. Readings were taken at increasing distances from 30 to 70 cm between the fixture and the spectral light meter. Tests were conducted under three conditions: “Open”, where the fixture emitted light to its surroundings; “Closed”, where the stand was closed off by wooden planks serving as walls; and “Foil”, where the same wooden planks were covered in foil on their inside.

**2.2. Chamber Design and Construction.** An illustration of the weathering chamber designed and built in this work is shown in Figure 1. The following section describes each component of the chamber with reference to the “Table of Components”.

The chamber consisted of two boxes. The “Light” box (A) was irradiated by UV rays, while the “Dark” box (B) sheltered

the samples from UV radiation. Both boxes consisted of a frame of wood scantlings with dimensions 0.6 m × 1.0 m × 0.6 m and 0.6 m × 0.6 m × 0.4 m, respectively, which were enclosed with plywood. The inside of the box was lined with aluminum foil to increase the irradiance inside the Light box.

Two Powerstar HQI-TS 250W/NDL Osram bulbs, “Bulb 1” and “Bulb 2”, irradiated the Light box. Each bulb was installed in a fixture (C) with an igniter and inductive ballast, which regulated current flow and voltage. The center of both bulbs was fixed to lay at the center of the box, ensuring equal distribution of UV radiation. Irradiance was measured with an OPTIMUM SRI-2000 Spectral Light Meter.

To ensure a stable temperature across both boxes, air was circulated from the Light box into the Dark box by means of three domestic extractor fans (D), each rated at 12 W each. These were connected to the Dark box using L-shaped poly(vinyl chloride) ducts (E). Cooler air from the Dark box was returned to the Light box by positive pressure through the return ducts (F). The temperature for each box was recorded using two UNI-T UT322 thermometers (G). The thermometers were placed on top of the boxes for display, while their thermocouple probes were suspended in the middle of each of the boxes. The temperature difference between both boxes was reduced by performing multiple temperature tests and sequentially installing additional stabilizing measures including an Arcadia 50 W Deep Heat Projector IR heater (H) in the Dark box, wrapping mineral wool around the ducts to reduce heat losses, and lining the dark box with foil and bubble wrap.

Apart from dry exposure, the weathering chamber also enabled the aeration of aqueous samples. Aeration was introduced using two Tetra APS 400 pumps (I), one assigned to each box. As shown in the Aqueous Sample Detail in Figure 1, each pump provided aeration through a series of silicon tubing of an internal diameter of 3 mm. Each tube was attached to a stainless steel straw (internal diameter 3 mm), which was submerged in the sand bed of aqueous samples. The aeration of each sample was controlled by individual pump valves whose airflow was set at 15 L/h. This simulates mechanical abrasion by the bombardment of sand particles that are present at the shore. All beakers (tall form, 600 mL) were filled with 500 mL of water, for a water column of 10 cm.

**2.3. Measuring Chamber Irradiance.** Another set of irradiance readings were taken after the chamber was constructed. The spectral meter was placed 60 cm away from the fixtures. Readings were taken at the center between each fixture, denoted as “Bulb 1” and “Bulb 2”. This was done for each fixture switched on individually and simultaneously.

**2.4. Finalizing Sample Distance.** The objective of this test was to finalize the sample distance that would yield the optimum irradiance values for the Mediterranean. Once more, the spectral meter was placed underneath the fixtures, which were switched on one at a time. Readings were taken with the distance between the meter and fixture reduced in steps. The desired UV-A irradiance was obtained at 35 cm from the fixture. Thus, the sample stand (J) was constructed upon which aqueous or dry samples (K) could be placed.

### 3. RESULTS AND DISCUSSION

**3.1. Bulb Selection.** Replicating solar radiation involves selecting a bulb that can emit wavelengths in magnitudes that reach the Earth’s surface. UV wavelengths range from 220 to 400 nm, subcategorized into UV-C (220–280 nm), UV-B (280–320 nm), and UV-A (320–400 nm).<sup>17</sup> UV-A irradiation

constitutes 95% of the UV radiation reaching the Earth’s surface, while the remaining 5% is attributed to UV-B. UV-C is completely absorbed by the ozone layer.<sup>17</sup> Irradiation can be measured by irradiance, defined as the radiant energy per unit time per unit surface area.<sup>18</sup> Total irradiance values (the summation of irradiance for UV and VIS wavelengths) for Malta average at 217 W m<sup>-2</sup>.<sup>19,20</sup> Separate irradiance values for UV-A and UV-B wavelengths are not available for Malta. The European light dosimeter network has found solar radiation to have a strong latitudinal dependence for countries between Sweden and the Canary Islands.<sup>21</sup> Thus, UV-A and UV-B values were extrapolated from Portugal at 20 and 0.72 W m<sup>-2</sup>, respectively.<sup>21</sup> Additionally, since Malta is located in the center of the Mediterranean Sea, its irradiance values are representative of the Mediterranean region.

Weathering protocols have advocated the use of xenon arc bulbs for exposure to photooxidation<sup>15</sup> due to their ability to simulate the solar radiation spectrum.<sup>17,22,23</sup> However, the pressure at which such bulbs operate poses safety concerns<sup>22</sup> within a chamber next to which an operator is working. While metal halide lamps are also highly pressurized, they are mounted within a secondary containment bulb which would contain any hot pieces of debris in the case of catastrophic failure.<sup>22</sup> This reduces the risk that xenon lamps would otherwise pose in a weathering chamber mainly composed of wood. As such, metal halide Powerstar HQI-TS 250W/NDL OSRAM bulbs were chosen to simulate Mediterranean solar conditions. According to their datasheet and as confirmed by the spectral spectrum obtained using the meter (Figure 2), emission of these bulbs spans from 350 nm up to 800 nm.<sup>24</sup>

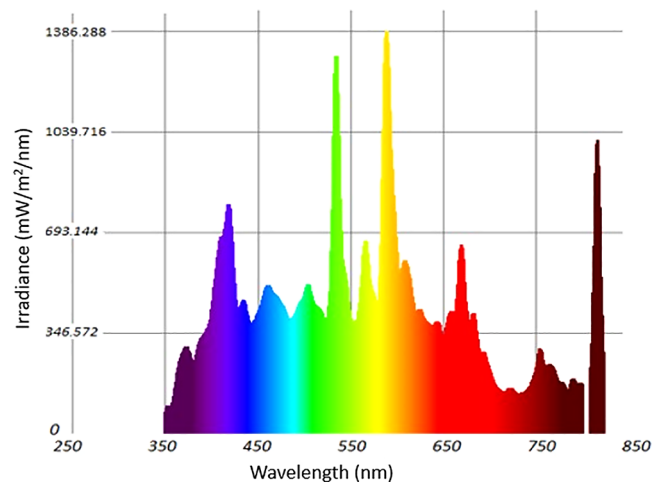


**Figure 2.** Spectrum of the metal halide bulb measured by a spectral light meter.

Thus, the bulb irradiated UV-A wavelengths (320–400 nm), which contribute to 95% of the UV irradiation reaching the Earth’s surface.<sup>25</sup> However, this means that the UV-B region (280–320 nm), which contributes to the last 5% of UV radiation that reaches the Earth’s surface, is excluded, leading to potentially milder weathering conditions.

**3.2. Understanding Bulb Behavior in Different Conditions.** The results of the irradiance test for the “Open” condition, described in Section 2.1, are displayed in Figure 3. As expected, the irradiance displayed an inverse square law behavior with increasing distance, as described in eq

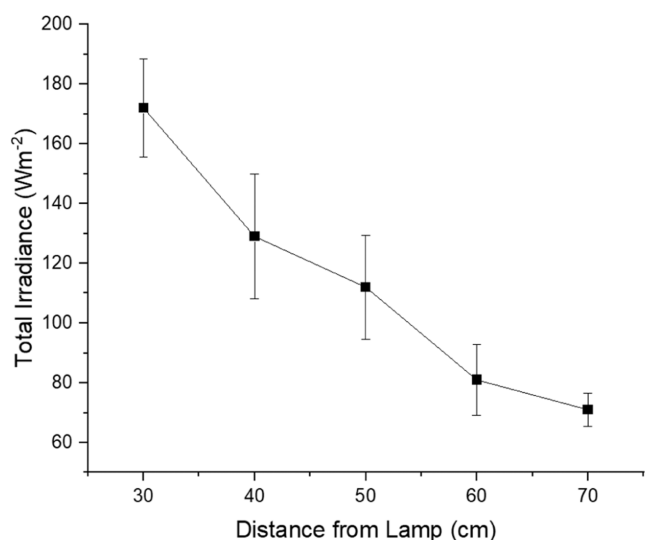


**Figure 3.** Variation of the total irradiance with distance from the metal halide lamp for the “Open” condition. Errors bars represent the standard deviation of 20 repeated readings.

1,<sup>26</sup> where  $E$  is the irradiance ( $\text{Wm}^{-2}$ ),  $I$  is the radiant flux ( $\text{W}$ ), and  $d$  is the distance from the source ( $\text{m}$ ).

$$E = \frac{I}{d^2} \quad (1)$$

The comparison of the “Open”, “Closed”, and “Foil” conditions can be seen in Figure 4. The data and error bars

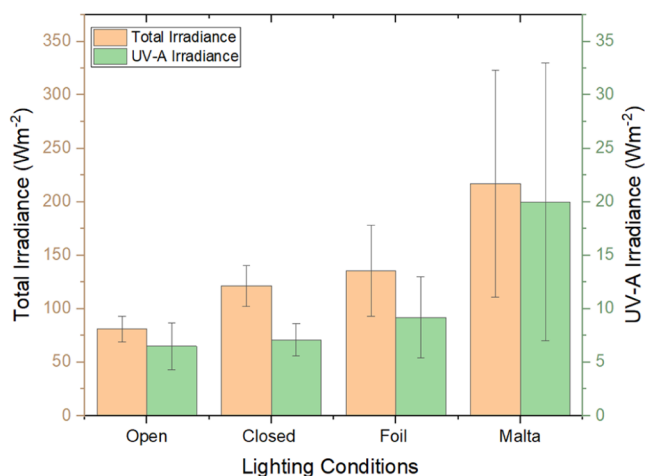


**Figure 4.** Results for the irradiance test conducted at 60 cm from the bulb for the “Open”, “Closed”, and “Foil” conditions. The data and error bars for Malta denote the range of irradiance throughout the year as reported in the literature.<sup>19</sup>

for “Malta”, acting as a representation of the Mediterranean region, denote actual readings throughout the year as reported in the literature.<sup>19</sup> As conditions varied from “Open” to “Closed” to “Foil”, an increase in the mean irradiance by 50% and a further 12% were detected, respectively. This showed that the enclosing walls and aluminum foil augmented irradiance in the setup through light reflection. The effects of aluminum foil on reflecting solar radiation were investigated by Tabaei and Ameri<sup>27</sup> whose results concluded that an aluminum foil reflector increased the output power of a photovoltaic module by 14%.

Ultimately, it was concluded that the chamber would be built at a height of 60 cm and incorporate two bulbs with internally lined foil. This enabled flexibility when finalizing the sample distance to provide the best compromise between simulating solar conditions for Malta (as an extrapolation for the Mediterranean), reducing reading variation, and minimizing the lab footprint taken up by the chamber.

**3.3. Measuring Chamber Irradiance.** The results obtained from measuring the chamber irradiance, described in Section 2.3, are displayed in Figure 5. “Only Bulb 1” and

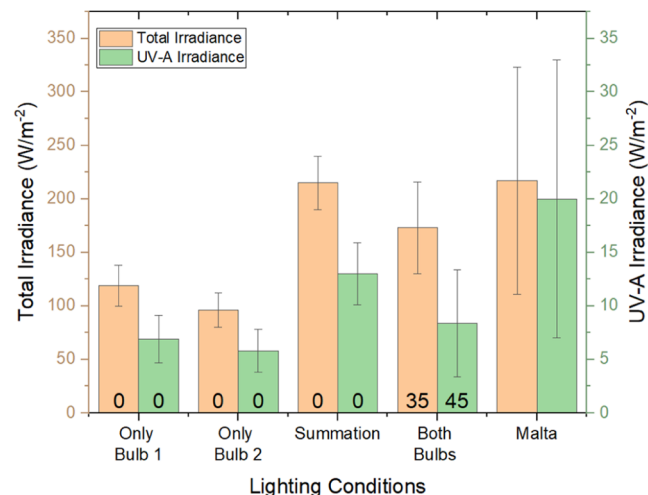


**Figure 5.** Results of the irradiance test conducted with the switch on individually and simultaneously inside the chamber. The data and error bars for Malta denote the range of irradiance throughout the year as reported in the literature.<sup>19</sup>

“Only Bulb 2” show the results obtained for each bulb switched on individually. “Summation” shows the mathematical summation of “Only Bulb 1” and “Only Bulb 2”. “Both Bulbs” shows the results for both bulbs switched on simultaneously. “Malta” shows the irradiance levels targeted to be simulated.<sup>19</sup> The numbers at the bottom of the column represent the number of oversaturation errors that occurred for each test condition. The “Summation” of “Only Bulb 1” and “Only Bulb 2” did not equate to the irradiance of “Both Bulbs” switched on simultaneously. This is because, although no oversaturation errors occurred when the bulbs were switched on individually, a high number of oversaturation errors occurred when both bulbs were switched on simultaneously. Such oversaturation errors resulted in a null reading being displayed by the meter. It was confirmed that the spectral meter had an upper limit of about  $1.5 \text{ W m}^{-2}$  of radiant energy for each individual wavelength. Following this, it was noted that whenever an oversaturation occurred for “Both Bulbs”, the peak within the 600 nm range (Figure 2) exceeded the  $1.5 \text{ W m}^{-2}$  limit. Since the oversaturation readings were not recordable, the readings reflected by “Both Bulbs” were lower than the actual irradiance within the chamber.

It was also observed that, while the total irradiance value of the “Summation” condition replicated the value for Malta (and hence the Mediterranean) accurately, the UV-A value of the chamber was low. Since UV radiation is more harmful than VIS radiation, replicating the UV-A irradiance of the Mediterranean accurately was prioritized. Hence, the sample distance was reestablished.

**3.4. Finalizing Sample Distance.** The results obtained from the test to finalize the sample distance (Section 2.4) are displayed in Figure 6. As discussed, bringing the meter closer

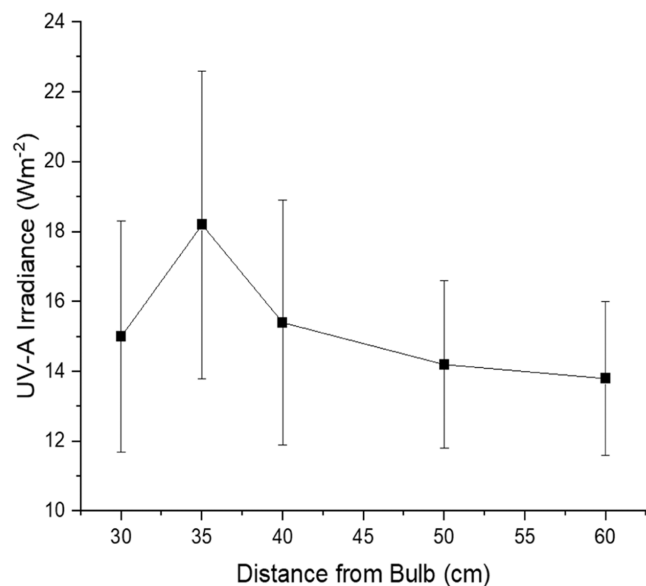


**Figure 6.** Variation of UV-A irradiance with distance from the bulbs in the weathering chamber.

to the bulbs resulted in higher irradiance. At 30 cm, oversaturation errors occurred, leading to lower irradiance readings. The optimum distance giving maximum irradiance without oversaturation was determined to be 35 cm from the bulbs. Therefore, a stand was constructed to place the samples 35 cm below the bulbs. The total irradiance and UV-A irradiance of the final system, illustrated in Figure 7, were 302



**Figure 7.** Interior of the “Light” box. Photograph taken by J. Galea.

$\pm 62$  and  $18.7 \pm 5.9 \text{ W m}^{-2}$  respectively. These values were comparable to Mediterranean values of 217 and  $20 \text{ W m}^{-2}$ , respectively.<sup>19,21</sup> Finally, readings were also taken across the boxes, and the irradiance varied by 2–3  $\text{W m}^{-2}$ . To compensate for such variations, the positions of all sample containers would be rotated every so often during weathering to ensure that all samples were being weathered equally.

**3.5. Temperature Regulation.** Studies show that an increase in temperature increases the rate of aging.<sup>28</sup> Hence, it was decided to increase the ambient temperature to accelerate the aging process. Tests and modifications to the chamber were made to ensure that the temperature conditions in the Light box and Dark box were consistent.

The final temperature readings, displayed in Table 1, were taken after the boxes were allowed to reach a stable

**Table 1. Temperature Tests to Bring the Light Box and Dark Box in Thermal Equilibrium**

stabilizing measures	light box temp. (°C)	dark box temp. (°C)	$\Delta$ temp. (°C)
2 extractor fans	47	37	10
3 extractor fans	47	41	6
IR heater	47	45	2
rockwool, bubble wrap, foil lining	47	47	0

temperature. Between each test, additional measures such as the introduction of extractor fans, IR heating, bubble wrap, mineral wool, and foil lining were sequentially introduced to bring the boxes to thermal equilibrium. Ultimately, the presence of two 250 W lamps within the confined chambers with all of the above-mentioned modifications generated a stable temperature of 47 °C in both chambers. It is acknowledged that this deviates from Maltese shore conditions; however, it should be appreciated that temperatures can reach these levels<sup>29</sup> and elevated temperatures result in accelerated weathering.<sup>28</sup>

**3.6. Aeration.** Several dry runs were conducted with the setup to observe the effects of aeration. During such tests, the environmental temperature of 47 °C caused complete evaporation of the sample water within 24 h. Cling film was placed over the beakers to minimize this (Figure 1, “Aqueous Sample Detail”), resulting in only 200 mL evaporating within 24 h. Thus, each beaker was topped up with 200 mL of DI water every day to compensate for the loss.

**3.7. Chemical and Physical Changes.** A comprehensive discussion of the chemical and physical aging induced by the setup is beyond the scope of this work. However, 90 days of UV exposure in this setup successfully resulted in the aging of the sample surface. The latter fragmented within 45 days, revealing a new surface with fresh properties. This coincided with other studies<sup>30–32</sup> that observed such cycles occur between 28 days (with more intense aging conditions) and 90 days (with less intense aging conditions).

Regarding physical changes, weathering setups have made use of both bubbling mechanisms and shaking tables to simulate tides. Within 90 days of weathering, the bubbling system used in this study induced holes and fibrils within the sample surface. These results resembled damage that was observed in polymers that weathered naturally in the sea.<sup>33</sup> On the other hand, when Reineccius et al.<sup>34</sup> made use of a shaking table to simulate tides, the sample surface became smoother after weathering. Bubbling may therefore cause sample surfaces to be bombarded with sand particles, inducing roughness and cracks, while shaking tables shift the sample surface back and forth on the sand bed, resulting in smoothening.

## 4. CONCLUSIONS

The aim of this work was to facilitate the accessibility of microplastic weathering setups. A weathering chamber was successfully constructed that replicated weathering conditions for Malta and, by extension, the Mediterranean. This chamber incorporated two boxes that could isolate and investigate the contribution of UV irradiation toward degradation. The chamber achieved UV-A irradiance values similar to those of the Mediterranean region. This chamber also incorporated agitation methods to simulate the mechanical abrasion that microplastics experience in the ocean. Furthermore, the temperature was successfully regulated between the Light and Dark conditions to maintain stable equilibrium. Such ad hoc setups present an attractive alternative to natural weathering or artificial weathering chambers as they encourage research teams with limited budgets to create their own setups and, consequently, act as a gateway to gather weathering data which is greatly needed for comparative purposes and to shed light on the fate, behavior, and toxicity of microplastics.

## AUTHOR INFORMATION

### Corresponding Author

**Sophie M. Briffa** – Department of Metallurgy and Materials Engineering, Faculty of Engineering, University of Malta, Msida MSD2080, Malta; [orcid.org/0000-0003-3064-4408](https://orcid.org/0000-0003-3064-4408); Email: [sophiebriffa@gmail.com](mailto:sophiebriffa@gmail.com)

### Authors

**Jack Galea** – Department of Metallurgy and Materials Engineering, Faculty of Engineering, University of Malta, Msida MSD2080, Malta

**Anthea Agius Anastasi** – Department of Metallurgy and Materials Engineering, Faculty of Engineering, University of Malta, Msida MSD2080, Malta

Complete contact information is available at:

<https://pubs.acs.org/10.1021/acsomega.4c03735>

### Notes

The authors declare no competing financial interest.

## ACKNOWLEDGMENTS

The authors acknowledge the project NanoFAB funded by “The transdisciplinary research and knowledge exchange (TRAKE) complex at the University of Malta (ERDF.01.124)” which is being cofinanced through the European Union through the European Regional Development Fund 2014–2020.

## REFERENCES

- (1) Peixoto, D.; Pinheiro, C.; Amorim, J.; Oliva-Teles, L.; Guilhermino, L.; Vieira, M. N. Microplastic Pollution in Commercial Salt for Human Consumption: A Review. *Estuarine, Coastal Shelf Sci.* **2019**, *219*, 161–168, DOI: 10.1016/j.ecss.2019.02.018.
- (2) Gambino, I.; Bagordo, F.; Grassi, T.; Panico, A.; De Donno, A. Occurrence of Microplastics in Tap and Bottled Water: Current Knowledge. *Int. J. Environ. Res. Public Health* **2022**, *19* (9), 5283 DOI: 10.3390/ijerph19095283.
- (3) Shruti, V. C.; Pérez-Guevara, F.; Elizalde-Martínez, I.; Kutralam-Muniasamy, G. First Study of Its Kind on the Microplastic Contamination of Soft Drinks, Cold Tea and Energy Drinks - Future Research and Environmental Considerations. *Sci. Total Environ.* **2020**, *726*, No. 138580.
- (4) Van Cauwenbergh, L.; Claessens, M.; Vandeghechuchte, M. B.; Janssen, C. R. Microplastics Are Taken up by Mussels (*Mytilus*

*Edulis*) and Lugworms (*Arenicola Marina*) Living in Natural Habitats. *Environ. Pollut.* **2015**, *199*, 10–17.

- (5) Oliveri Conti, G.; Ferrante, M.; Banni, M.; Favara, C.; Nicolosi, I.; Cristaldi, A.; Fiore, M.; Zuccarello, P. Micro- and Nano-Plastics in Edible Fruit and Vegetables. The First Diet Risks Assessment for the General Population. *Environ. Res.* **2020**, *187*, No. 109677.

- (6) Blackburn, K.; Green, D. The Potential Effects of Microplastics on Human Health: What Is Known and What Is Unknown. *Ambio* **2022**, *51* (3), 518–530.

- (7) Hwang, J.; Choi, D.; Han, S.; Choi, J.; Hong, J. An Assessment of the Toxicity of Polypropylene Microplastics in Human Derived Cells. *Sci. Total Environ.* **2019**, *684*, 657–669.

- (8) Peretz, J.; Vrooman, L.; Ricke, W. A.; Hunt, P. A.; Ehrlich, S.; Hauser, R.; Padmanabhan, V.; Taylor, H. S.; Swan, S. H.; VandeVoort, C. A.; Flaws, J. A. Bisphenol A and Reproductive Health: Update of Experimental and Human Evidence, 2007–2013. *Environ. Health Perspect.* **2014**, *122* (8), 775–786.

- (9) Lucas, N.; Bienaime, C.; Belloy, C.; Queneudec, M.; Silvestre, F.; Nava-Saucedo, J.-E. Polymer Biodegradation: Mechanisms and Estimation Techniques – A Review. *Chemosphere* **2008**, *73* (4), 429–442.

- (10) Crawford, C. B.; Quinn, B. Physicochemical Properties and Degradation. In *Microplastic Pollutants*; Elsevier, 2017; pp 57–100.

- (11) Kershaw, P. J.; Rochman, C. M. *Sources, Fate and Effects of Microplastics in the Marine Environment: Part 2 of a Global Assessment. Reports and Studies-IMO/FAO/Unesco-IOC/WMO/IAEA/UN/UNEP Joint Group of Experts on the Scientific Aspects of Marine Environmental Protection (GESAMP) Eng No. 93* 2016.

- (12) Koelmans, B.; Pahl, S.; Backhaus, T. et al. *A Scientific Perspective on Microplastics in Nature and Society*; SAPEA: Berlin, 2019; p 173.

- (13) Cowger, W.; Booth, A. M.; Hamilton, B. M.; Thaysen, C.; Primpke, S.; Munno, K.; Lusher, A. L.; Dehaut, A.; Vaz, V. P.; Liboiron, M.; Devriese, L. I.; Hermabessiere, L.; Rochman, C.; Athey, S. N.; Lynch, J. M.; De Frond, H.; Gray, A.; Jones, O. A. H.; Brander, S.; Steele, C.; Moore, S.; Sanchez, A.; Nel, H. Reporting Guidelines to Increase the Reproducibility and Comparability of Research on Microplastics. *Appl. Spectrosc.* **2020**, *74* (9), 1066–1077.

- (14) De Ruijter, V. N.; Redondo-Hasselerharm, P. E.; Gouin, T.; Koelmans, A. A. Quality Criteria for Microplastic Effect Studies in the Context of Risk Assessment: A Critical Review. *Environ. Sci. Technol.* **2020**, *54* (19), 11692–11705.

- (15) Alimi, O. S.; Claveau-Mallet, D.; Kurusu, R. S.; Lapointe, M.; Bayen, S.; Tufenkji, N. Weathering Pathways and Protocols for Environmentally Relevant Microplastics and Nanoplastics: What Are We Missing? *J. Hazard. Mater.* **2022**, *423*, No. 126955.

- (16) Andrade, J.; Fernández-González, V.; López-Mahía, P.; Muniategui, S. A Low-Cost System to Simulate Environmental Microplastic Weathering. *Mar. Pollut. Bull.* **2019**, *149*, No. 110663.

- (17) Behar-Cohen, F.; Baillet, G.; De Agyuavives, T.; et al. Ultraviolet Damage to the Eye Revisited: Eye-Sun Protection Factor (E-SPF), a New Ultraviolet Protection Label for Eyewear. *Clin. Ophthalmol.* **2014**, *8*, 87–104, DOI: 10.2147/OPHTH.S46189.

- (18) Frederick, J. E. Ozone Depletion and Related Topics | Ozone as a UV Filter. In *Encyclopedia of Atmospheric Sciences*; Elsevier, 2015; pp 359–363.

- (19) Galdies, C. Potential Future Climatic Conditions on Tourists: A Case Study Focusing on Malta and Venice. *J. Malta Chamber Sci.* **2015**, No. 2, 86–104, DOI: 10.7423/XJENZA.2015.2.01.

- (20) Solar Resource Maps and GIS data for 200+ Countries | Solargis. <https://solargis.com/maps-and-gis-data/download/malta>. (accessed Apr 7, 2023).

- (21) Häder, D.-P.; Lebert, M.; Colombetti, G.; Figueroa, F. European Light Dosimeter Network (ELDONET): 1998 Data. *Helgol. Mar. Res.* **2001**, *55* (1), 35–44, DOI: 10.1007/s101520000059.

- (22) Dong, X.; Sun, Z.; Nathan, G. J.; Ashman, P. J.; Gu, D. Time-Resolved Spectra of Solar Simulators Employing Metal Halide and Xenon Arc Lamps. *Sol. Energy* **2015**, *115*, 613–620.

- (23) Presciutti, A.; Asdrubali, F.; Marrocchi, A.; Broggi, A.; Pizzoli, G.; Damiani, A. Sun Simulators: Development of an Innovative Low Cost Film Filter. *Sustainability* **2014**, *6* (10), 6830–6846.
- (24) POWERSTAR HQI-TS. <https://www.ledvance.com/professional/products/lamps/high-intensity-discharge-lamps/metal-halide-lamps-with-quartz-technology/powerstar-hqir-ts-c7286>. (accessed June 24, 2024).
- (25) Radiation: Ultraviolet (UV) Radiation. [https://www.who.int/news-room/questions-and-answers/item/radiation-ultraviolet-\(uv\)](https://www.who.int/news-room/questions-and-answers/item/radiation-ultraviolet-(uv)). (accessed Mar 23, 2023).
- (26) Ryer, A. *Light Measurement Handbook*; International Light: Newburyport, MA, 1997.
- (27) Tabaei, H.; Ameri, M. The Effect of Booster Reflectors on the Photovoltaic Water Pumping System Performance. *J. Sol. Energy Eng.* **2012**, *134* (1), No. 014501.
- (28) Briffa, S. M.; Lynch, I.; Trouillet, V.; Bruns, M.; Hapiuk, D.; Valsami-Jones, E. Thermal Transformations of Manufactured Nanomaterials as a Proposed Proxy for Ageing. *Environ. Sci.: Nano* **2018**, *5* (7), 1618–1627.
- (29) Europe Braces for Sweltering July. [https://www.esa.int/Applications/Observing\\_the\\_Earth/Copernicus/Sentinel-3/Europe\\_braces\\_for\\_sweltering\\_July](https://www.esa.int/Applications/Observing_the_Earth/Copernicus/Sentinel-3/Europe_braces_for_sweltering_July). (accessed Mar 13, 2024).
- (30) Reineccius, J.; Schönke, M.; Waniek, J. J. Abiotic Long-Term Simulation of Microplastic Weathering Pathways under Different Aqueous Conditions. *Environ. Sci. Technol.* **2023**, *57* (2), 963–975.
- (31) Fernández-González, V.; Andrade-Garda, J. M.; López-Mahía, P.; Muniategui-Lorenzo, S. Impact of Weathering on the Chemical Identification of Microplastics from Usual Packaging Polymers in the Marine Environment. *Anal. Chim. Acta* **2021**, *1142*, 179–188.
- (32) Conradie, W.; Dorfling, C.; Chimphango, A.; Booth, A. M.; Sørensen, L.; Akdogan, G. Investigating the Physicochemical Property Changes of Plastic Packaging Exposed to UV Irradiation and Different Aqueous Environments. *Microplastics* **2022**, *1* (3), 456–476.
- (33) Ioakeimidis, C.; Fotopoulou, K. N.; Karapanagioti, H. K.; Geraga, M.; Zeri, C.; Papatheodorou, E.; Galgani, F.; Papatheodorou, G. The Degradation Potential of PET Bottles in the Marine Environment: An ATR-FTIR Based Approach. *Sci. Rep.* **2016**, *6* (1), No. 23501.
- (34) Abiotic Long-Term Simulation of Microplastic Weathering Pathways under Different Aqueous Conditions | Environmental Science & Technology. <https://pubs.acs.org/doi/full/10.1021/acs.est.2c05746>. (accessed Mar 29, 2023).